FINITE ELEMENT ELECTROMAGNETIC 2D MODEL OF AN EDDY CURRENT HEATER WITH ROTATING PERMANENT MAGNETS

Virgiliu FIREȚEANU, Onur NEBI

POLITEHNICA University of Bucharest/Faculty of Electrical Engineering/EPM_NM Laboratory, Bucharest, Romania
firetean@amotion.pub.ro

***Abstract* - The paper investigates a simply device called Permanent Magnet Eddy Current Heater able to transform the rotation mechanical energy into heat. This study is based on a 2D finite element model of the electromagnetic field, which takes into account the field - rotating motion coupling.**
The accuracy of the step by step in time domain solution with respect to the time variable is studied. The dependences of induced power on rotor speed and on number of poles are analyzed.

Keywords: *eddy current heater, finite element analysis, permanent magnet rotating field.*

1. INTRODUCTION

In the last period the humanity is more and more interested in the use of clean energy resources like the wind energy or water flow energy. The mechanical energy associated with such energy sources is generally converted into electrical energy, this option being determined by the flexibility of transportation and distribution of this type of energy. An important part of the electrical energy is used in applications based on electricity conversion into heat, and in many cases the users are located in the same area where the potential of wind or water flow energy is comparable with the needs of heat. That is why the conversion of the mechanical energy produced by wind or water turbine into heat can be advantageous in comparison with the usual double conversion scheme mechanical energy - electrical energy - heat. This paper studies a device called Permanent Magnet Eddy Current Heater (PM-ECH), Figure 1, whose rotor is coupled to the turbine and the stator is the heating element - part of the heater where the fluid is used for heat transport to the user.
The PM-ECH rotor consists in an inner magnetic core surrounded by an even number of magnets, which generates at the rotor periphery a heteropolar magnetic field. The stator armature is composed by an inner tube, magnetic steel made and an outer annular chamber in which flows the fluid to be heated. The PM-ECH operating principle is very simply. The rotor motion generates eddy currents in the magnetic steel tube of the stator, respectively generates heat in this tube as the result of the Joule effect of these currents. Consequently, the stator magnetic tube has a triple function: magnetic core with respect to the magnetic field generated by the rotor, solid conductor with respect to the eddy currents, and heating element with respect to the fluid to be heated.

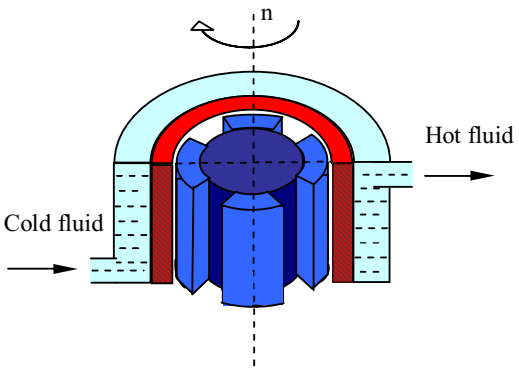

Figure 1: PM-ECH principle.

This paper presents a 2D finite element model of the PM-ECH device modeled with FLUX2D software. The magnetic field and the induced currents are computed, the influence of the rotor speed and of the number of poles on the induced power are analyzed.

2. MATHEMATICAL MODEL

The electromagnetic field in the PM-ECH device is governed by the differential equation:

$$\text{curl}\,[(1/\mu)\text{curl}A] + \sigma(\partial A/\partial t) = \text{curl}\,(Br/\mu) \qquad (1)$$

where μ is the magnetic permeability and σ is the electric conductivity, **A** - the magnetic vector potential is the state variable of the unknown electromagnetic field and $\mathbf{B}_r$ is the remanent magnetic flux density of the magnets, which represent the source of the magnetic field. The second term in the left side of the equation (1) represents the eddy current density.
The equation (1) has particular form in the different regions of the device, which are:

(a) magnetic core of the rotor - a magnetic non-linear region, non-conductive ($\sigma = 0$) and no magnet ($B_r = 0$);

(b) permanent magnets - magnetic linear ($\mu_r \neq 1$), non-conductive and with $B_r \neq 0$ regions;

(c) rotor-stator air gap - a non-magnetic region ($\mu_r = 1$), non-conductive and no magnet;

(d) stator tube - eddy current region, magnetic non-linear, conductive ($\sigma \neq 0$) and no magnet.

The magnetic potential unknown in the stator coordinate system is space and time dependent, $\mathbf{A}(\mathbf{r}, t)$, because the position of the rotor with respect to the stator is time dependent. For rotor motion with imposed value of speed, the integration of equation (1) with respect to the time variable t is based on step by step in time domain method until the device reaches the steady state operation regime. Usually, the initial condition $\mathbf{A}(\mathbf{r}, 0) = 0$ is considered. The numerical solution of the space structure of the electromagnetic field for any time step is a finite element solution. In the 2D plane model considered in this paper, the source $\mathbf{B}_r$ of the electromagnetic field is a vector in the plane of the computation domain (x, y). In the stator cartesian coordinate system (x, y, z), the structure of this vector is $\mathbf{B}_r$ [$B_{rx}(x,y,t)$ $B_{ry}(x,y,t)$ 0]. As consequence, the vector of the magnetic potential is oriented along the Oz axis, i.e. $\mathbf{A}$ [0 0 A(x,y,t)].

3. GEOMETRY, MESH and PHYSICAL PROPERTIES

3.1. Geometry and mesh of the electromagnetic field computation domain

The device studied is characterized by the value of 40 mm for the inner diameter of the rotor magnetic core, 120 mm for the outer diameter of the rotor magnetic core, 160 mm for the outer diameter of the rotor, 1 mm for the air gap thickness, 220 mm for the outer diameter and 300 mm for the heater height.

The surface regions of the computation domain in Figure 2 a) are as follows:

- ROTOR, the rotor magnetic core;
- MAGNET_PLUS, three permanent magnets with radial positive magnetization;
- -MAGNET_MINUS, three permanent magnets with radial negative magnetization;
- AIRGAP, the air gap between rotor and stator;
- STATOR, the region where the induced currents are generated;
- AIR, the rest of the computation domain surface.

The line regions ROTOR_INT - the inner circle of the rotor magnetic core and STATOR_EXT - the outer circle of the stator are boundaries of the computation domain on which the condition of null local value of the magnetic flux is considered.

The main feature in the generation of finite element meshing of the computation domain, Figure 2 b) concerns the area of the stator region toward the air gap. The stator is a region of solid conductor type and this area is characterized by maximum values and maximum variation of induced current density. The mesh of computation domain is 2nd order type and it has 7400 surface elements.

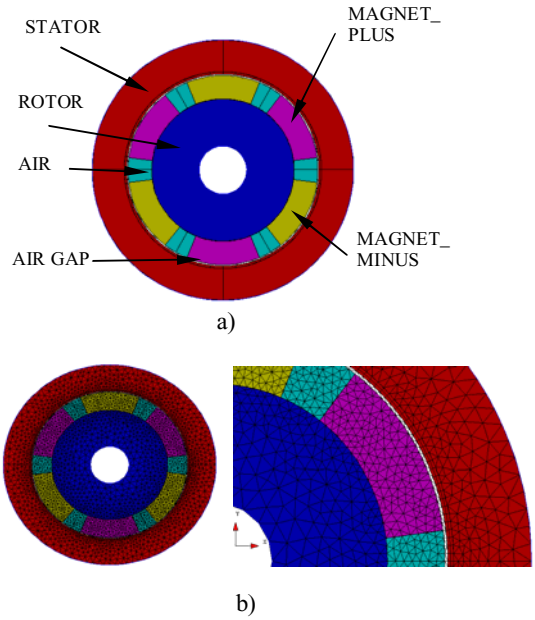

Figure 2: Computation domain of electromagnetic field for 6 poles PM-ECH (a) and mesh (b).

3.2. Physical properties

The material of the ROTOR region is represented by magnetic non-linear laminations, with B(H) curve presented in Figure 3, defined by the saturation $B_s = 2$ T and initial magnetic relative permeability $\mu_{ri} = 4000$.

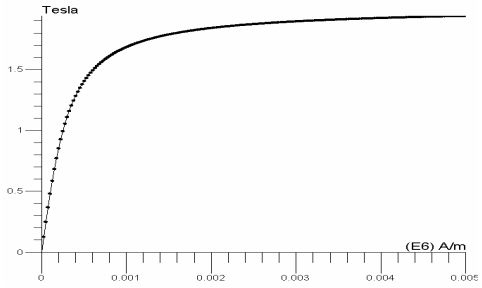

Figure 3: B(H) dependence of rotor magnetic core laminations.

The magnets placed on the rotor, defined by the remanent flux density $B_r = 1$ T and the relative permeability $\mu_r = 1.1$, are radial magnetized.

The stator is magnetic non-linear steel made, characterized by the saturation $B_s = 1.9$ T, the initial

magnetic relative permeability μ_{ri} = 2000 and the electrical conductivity σ = 0.5 $\mu\Omega$m.
Motion properties assigned to different part of the device are as follows:

- ROTATING set includes the regions: ROTOR, MAGNET_PLUS, MAGNET_MINUS and AIR;
- FIXED set is represented by the STATOR region;
- COMPRESSED set is the AIRGAP region.

4. RESULT ANALYSIS

4.1. Influence of time step value on numerical results accuracy

The solution of the equation (1) with respect to the variable time t is obtained by the method called step by step in time domain. The continuous rotating motion of the mechanical set ROTATING with an imposed speed n is simulated by successive positions of the rotor with respect to the stator defined by the angular step $\Delta\alpha = (2\pi n/60)\cdot\Delta t$, where Δt is the time step.
For a numerical application with 2p = 2 poles and rotor speed n = 1200 rpm, the analyze of the simulation results show that the transient state of the electromagnetic field is finished after 0.1496 seconds. Taking into account the values 0.8 ms, 0.4 ms, 0.2 ms and 0.1 ms for the time step Δt, respectively the corresponding angular step values $\Delta\alpha$, there are presented in Table 1 the numerical steady state results of the induced power P in the stator, the corresponding electromagnetic torque M, the maximum values of the magnetic flux density B_δ in the air gap and the induced current density in the stator. The differences between the current results and that marked in the previous row, expressed in percent, shows the influence of the time step value on the accuracy of the numerical results. This accuracy increases when the time step decreases, but the computation time, which depends on the number of steps, increases also. The computation time for PC is around 30 minutes for a Intel Core 2 CPU, at 2.13GHz processor and 2GB of RAM.

Δt [ms]	$\Delta\alpha$ [deg]	P [kW]	$B_{\delta max}$ [T]	J_{max} [A/mm^2]	M [Nm]
0.8	5.76	54.48	1.089	15.40	427.94
0.4	2.88	56.16 +3.08%	1.104 +1.38%	15.98 +3.76 %	443.90 +3.73%
0.2	1.44	57.04 +1.57%	1.111 +0.63%	16.32 +2.12 %	452.11 +1.85%
0.1	0.72	57.55 +0.89%	1.114 +0.27%	16.51 +1.16 %	456.20 +0.90%

Table 1: Time step and the results accuracy.

4.2. Dependence of induced power on rotor speed

The results for the two poles of PM_ECH device presented in Table 2 and graphically presented in Figure 4, shows the increase of the induced power when the rotor speed increases. For low speed range [0, 600] rpm a parabolic increase of the induced power can be considered. Taking into account the results for 200 rpm and 400 rpm, the power dependence on speed can be expressed by the formula:

$$P = 9.57\cdot10^{-5}\cdot n^{1.977} \quad (2)$$

Over 600 rpm, a line can approximate the increase of the induced power when rotor speed increases. Taking into account the results for 800 rpm and 1000 rpm, the power dependence on speed can be expressed by the following line:

$$P = 4.84\cdot10^{-2}\cdot n \quad (3)$$

n [rpm]	0	200	400	600	800	1000	1200
P [kW]	0	3.40	13.39	26.89	37.04	46.73	56.13

Table 2: Rotor speed and the induced power.

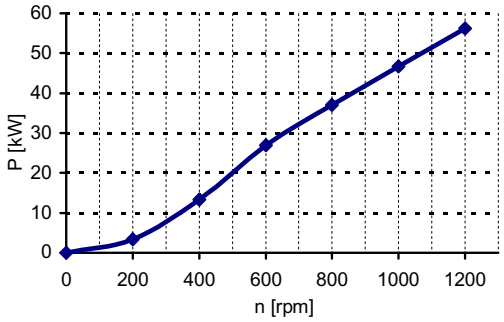

Figure 4: Dependence of induced power on rotor speed.

4.3. The induced power and the number of rotor poles

As the numerical results in Table 3 or their graphical representation in Figure 5 shows, there is an optimum of the number of poles with respect to the value of device power. These results correspond to the rotor speed 1000 rpm and the most convenient number of rotor poles, 2p = 4.

Nb. poles	2	4	6	8
P [kW]	46.73	65.37	50.42	34.38

Table 3: The number of poles on the induced power.

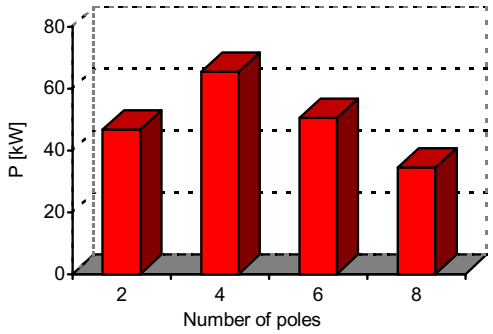

Figure 5: Dependence of device power on number of poles.

4.4. Graphical results

The frequency of the induced currents corresponding to 2p = 4 poles and the rotor speed n = 1000 rpm has the value f = pn/30 = 33.33 Hz. The value $\Delta t = 0.24$ ms for the time step was considered. Figure 6 shows the transient variation of the induced power. After about 40 ms, respectively after 40/0.24 = 167 time steps, the steady state is reached. The results below correspond to the final time step, respectively to the end of the study, $t_f = 60$ ms.

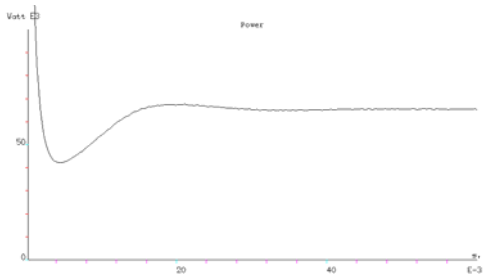

Figure 6: Transient variation of the induced power.

The lines of the magnetic field and the chart of the magnetic flux density are presented in Figure 7. The penetration of magnetic field in the stator is important, because the degree of the magnetic saturation of this region is very high.

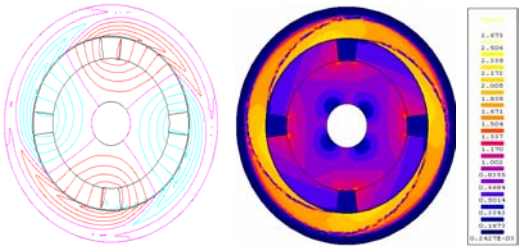

Figure 7: Lines and chart of the magnetic field.

The abscissa direction in Figure 8, where the variation of the normal and tangent components of the magnetic flux density along the middle circle of the air gap are presented, is the same with the rotor counterclockwise motion. With respect to the rotor, the magnetic flux density in the air gap has an important increase from the entry extremity to the exit extremity of the magnets. This means that the reaction of the magnetic field generated by the induced currents is very important.

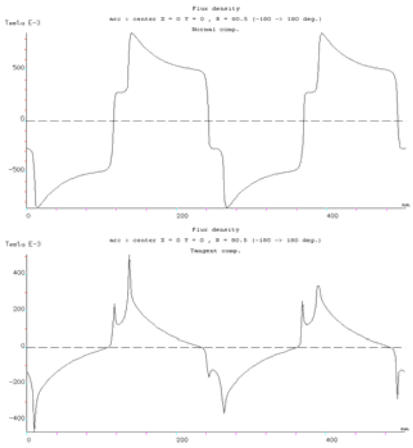

Figure 8: Radial and tangential components of the magnetic flux density.

From the chart in Figure 9 a) a value of about 10 A/mm^2 of the maximum rms value of the induced current density can be estimated. The variation of the induced current density along a circle on the inner surface of the stator is presented in Figure 9 b).

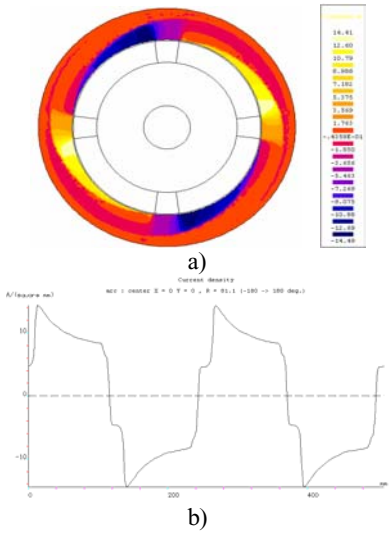

a)

b)

Figure 9: Induced current density chart (a) and the variation along the inner stator surface (b).

The time variation of the induced current density in a point near the inner surface of the stator and the harmonic spectrum of this current are presented in Figure 10. The coordinates of the point are x = 81.1 mm and y = 0 mm. The harmonic spectrum of the induced current is presented for one period, from 190 ms to 390 ms.

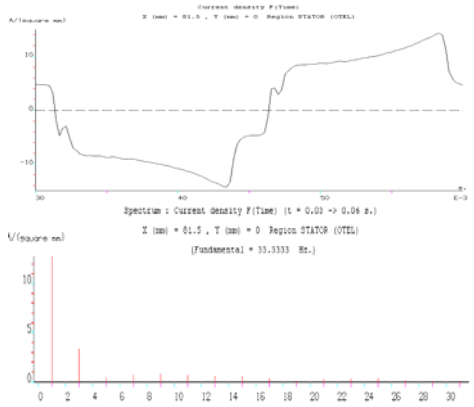

Figure 10: Quasi state time variation of the induced current density.

The chart of the induced power density in the stator region, respectively the variation of this quantity along a circle on the inner surface of the stator, are presented in Figure 11.

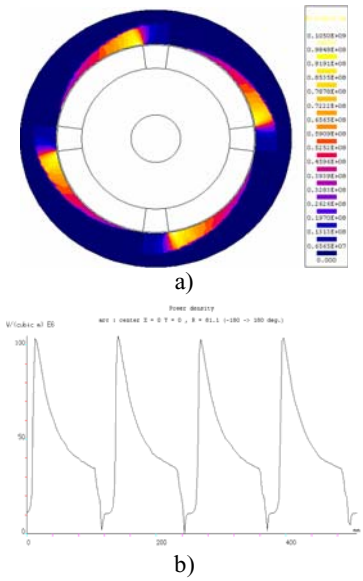

Figure 11: Induced power density chart (a) and the variation along the inner stator surface (b).

The Figures 12 and 13 contains the lines of the magnetic field and the chart of the current density in the PM_ECH device with different number of poles 2p = 2, 4, 6, 8. Since the rotor speed is 1000 rpm, the corresponding values of the frequency of the induced currents are 16.7, 33.3, 50.0, and 66.7 Hz. Comparing the different images, it result that the thickness of the stator must be correlated with the number of poles. The thickness must decrease when the number of poles increases.

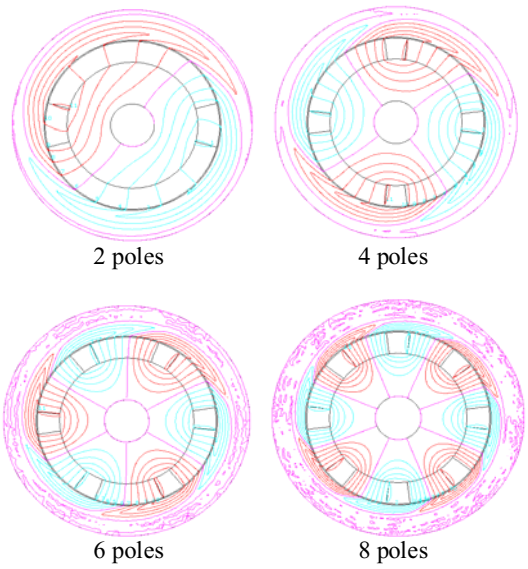

Figure 12: Lines of the magnetic flux density.

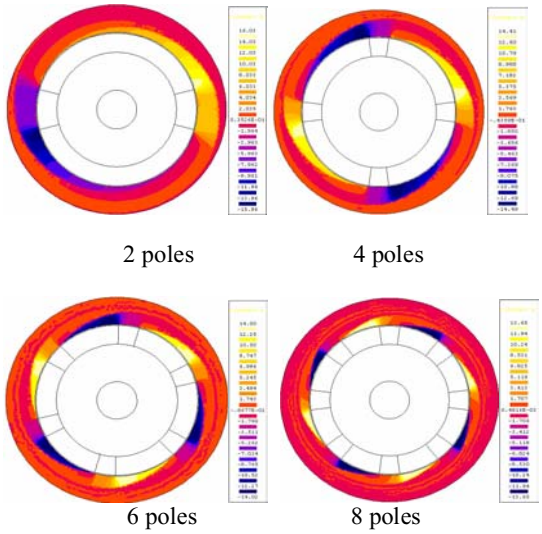

Figure 13: Chart of the induced current density.

The results in Table 4 of an application with two poles and the rotor speed 1000 rpm, respectively the corresponding dependence of the induced power P on the stator thickness, a, Figure 14, show as optimum the value a_o = 16 mm.

a[mm]	21	16	15	14	11
P[kW]	46.73	46.34	43.44	39.61	28.14

Table 4: The stator thickness on induced power.

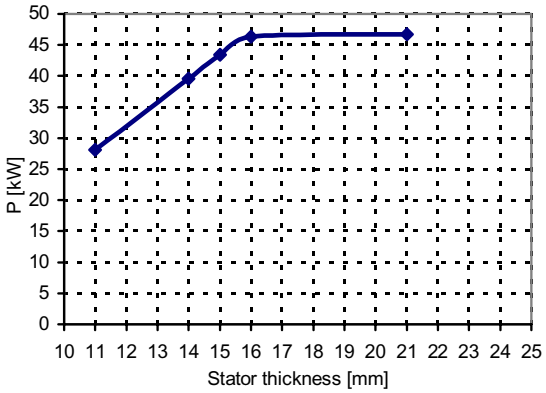

Figure 14: Induced power dependence on the stator thickness.

The charts of current density in Figure 15, explain why if the stator thickness decreases under the optimal value the induced power decreases. When the stator thickness decreases under the maximum of induced currents penetration, whose value is the optimum a_o, the area of the stator cross-section generating induced power becomes more and more reduced.

5. CONCLUSIONS

The optimal design of the Permanent Magnet Eddy Current Heater must take into account the first important finding of this paper, respectively the correlation speed - number of poles, for which the maximum power is obtained. The second important result is the optimum value of the stator thickness, i.e. the value under which the induced power decreases and starting from which the induced power remains constant when the stator thickness increases.

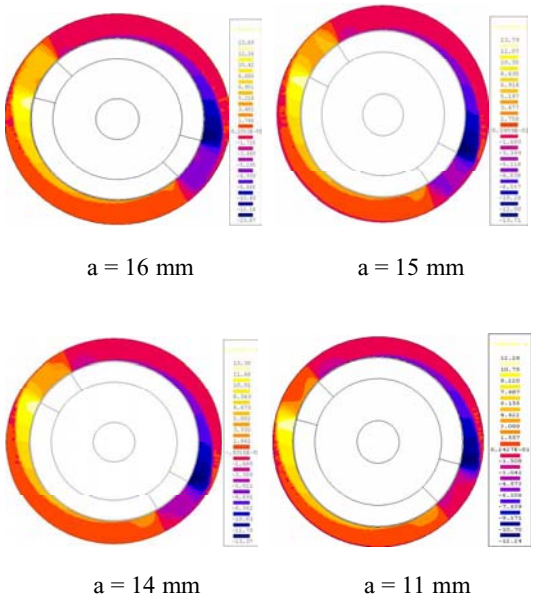

Figure 15: Chart of the induced currents for different values of the stator thickness.

References

[1] A.B.J. Reece and T.W. Preston, *Finite element methods in electrical power engineering,* Oxford Science Publications (2000);

[2] R. Araneo, A. Geri, M. Maccioni, G.M. Veca, *Eddy Current induction heating of a conducting cylinder in a magnetic field*, Proc. of International Symposium on Heating by Electromagnetic Sources, Padua, June 19-22, 2007;

[3] V. Fireţeanu, T. Tudorache, M. Popa, S. Paşca, *Finite Element Analysis of Aluminum Billet Heating by Rotation in DC Magnetic Fields*, Proc. of XXIV UIE International Congress, Krakow, May 19-22, 2008.